Article

Long-Term Pterostilbene Supplementation of a High-Fat Diet Increases Adiponectin Expression in the Subcutaneous White Adipose Tissue

Sofia Parrasia [1,2,†], Eva Galletta [1,2,†], Martina La Spina [1,†], Arianna Magrini [1,3], Michele Azzolini [1,‡], Marika Salvalaio [4] and Lucia Biasutto [1,3,*]

1   Department of Biomedical Sciences, University of Padova, 35131 Padova, Italy; sofia.parrasia@unipd.it (S.P.); eva.galletta@bio.unipd.it (E.G.); martina.spina@bio.unipd.it (M.L.S.); ariannamagrina@gmail.com (A.M.); michele.azzolini@gmail.com (M.A.)
2   Department of Biology, University of Padova, 35131 Padova, Italy
3   CNR Neuroscience Institute, 35131 Padova, Italy
4   Department of Pharmaceutical and Pharmacological Sciences, University of Padova, 35131 Padova, Italy; marika.salvalaio@unipd.it
*   Correspondence: lucia.biasutto@cnr.it; Tel.: +39-049-827-6054
†   These authors contributed equally to this work.
‡   Current address: Department of Physiology and Pharmacology, Karolinska Institutet, 171 77 Stockholm, Sweden.

Abstract: Pterostilbene (Pt) is a natural phenol found in blueberries and grapes; it shows remarkable biomedical activities similar to those of resveratrol, but its higher bioavailability is a major advantage for possible biomedical applications. Our group has recently demonstrated that long-term (30 weeks) administration of Pt to mice maintained on a high-fat diet counters weight gain and promotes browning of subcutaneous white adipose tissue (sWAT). By Real-time quantitative PCR and Western Blot analysis of the sWAT and visceral white adipose tissue (vWAT) from the same mice used in the previous study, we show here that Pt induced a long-term increase of Adiponectin, Interleukin 10 and of M2 macrophage marker Cd206. The effects were observed in sWAT, while no significant changes were detected in vWAT. The process taking place seems to mimic that occurring in sWAT during cold-induced browning. Analysis of a few pro-inflammatory cytokines (Interleukin 6, Tumor necrosis factor α) and of the NFkB pathway did not reveal marked effects of Pt supplementation. In summary, the mechanisms and processes through which Pt acts in adipose tissue appear to closely mimic those set in motion by cold-induced browning, and point to a possible impact of experimental conditions in the final output of a nutraceutical intervention.

Keywords: pterostilbene; C57BL/6 mice; Adiponectin; white adipose tissue; diet-induced obesity; browning

1. Introduction

Pterostilbene (Pt) is a plant phenol, differing from its most popular analog, resveratrol, because two of the three hydroxyl groups of the molecule are methylated. This imparts higher lipophilicity and bioavailability, and thus efficacy. In fact, Pt shows a variety of health promoting properties [1–3]; its prolonged consumption has been reported to exert beneficial effects also against obesity [4–8].

We previously demonstrated that long-term (30 weeks) administration of Pt to mice maintained on a high-fat diet countered weight gain and promoted browning of subcutaneous adipose tissue (sWAT) [5].

Brown Adipose Tissue (BAT) is an inducible mammalian organ providing non-shivering thermogenesis, i.e., turning food-derived energy into heat [9,10]. The process of "browning" is characterized by the formation of thermogenic "beige" adipocytes in subcutaneous

white adipose tissue, and is considered a hopeful approach to the problem of obesity in modern societies [11,12]. Beige adipocytes express a set of specific genes, but also brown adipocyte-associated genes such as *Ucp1*, and have features in common with brown cells, such as abundant mitochondria. Physiological factors inducing browning are, for example, exposure to cold [13], physical exercise [14,15], or thyroid hormones [16,17]. Cold exposure leads to the release of norepinephrine by the sympathetic nervous system, which leads to activation of β3-adrenergic signalling; downstream signalling then branches and interacts with other pathways in complex patterns [18–20]. A key feature of cold-induced browning in mice is Adiponectin elevation in subcutaneous fat deposits (but not in epididymal WAT or interscapular BAT) [21,22], which persists for at least weeks. Of note, circulating Adiponectin instead decreases, and intravenously-injected Adiponectin accumulates in sWAT [23].

Cytokines released by immune cells in the adipose tissue play a crucial role in adipose tissue homeostasis. They regulate the thermogenic activity of brown and beige adipocytes [24] (i.e., Interleukin 4, Interleukin 13 [25,26]), but also contribute to the low grade chronic inflammatory state commonly observed during obesity [27,28], which in turn is implicated in the development of obesity-related comorbidities such as insulin resistance, type 2 diabetes, or cardiovascular disease. Tumor necrosis factor (TNFα), for example, is a pro-inflammatory cytokine, but it has also been reported to increase upon exposure to low temperatures [29,30]. Interleukin 6 (IL6), which can act as a pro-inflammatory cytokine or an anti-inflammatory myokine, has been reported to increase about 6-fold upon exposure to cold (4 °C; 15 days) [29]. Non-shivering thermoregulation is impaired in IL6-deficient mice [31–33].

In this work, we wanted to investigate the impact of Pt on the expression of Adiponectin and a few anti and pro- inflammatory markers in two different adipose tissue depots: the subcutaneous (inguinal) WAT (sWAT), which is the most prone to browning, and the visceral (epididymal/periovaric) one (vWAT), which has been reported to be the most affected by chronic inflammation during obesity. Importantly, the experimental design included both males and females [34–36]. The results we obtained highlighted that Pt has an effect on the sWAT which resembles that induced by cold exposure, and points out that the beneficial effects of Pt in our experimental model are mediated by mechanisms other than an anti-inflammatory effect on vWAT.

2. Materials and Methods

2.1. Animals

C57BL/6 mice were housed in the SPF (specific pathogen free) facility of the Department of Pharmaceutical and Pharmacological Sciences (Padova, Italy); food and water were provided ad libitum. Procedures were all approved by the University of Padova Ethical Committee for Animal Welfare (OPBA) and by the Italian Ministry of Health (Permit Number 211/2015-PR), and conducted with the supervision of the Central Veterinary Service of the University of Padova, in compliance with Italian Law DL 26/2014, embodying UE Directive 2010/63/EU.

2.2. Animal Treatments

Animal cohort was the same used in [5]; briefly, 1 month after birth (i.e., after weaning), mice were divided in three experimental groups (16 animals/group; 8 males and 8 females): the STD group was fed a standard diet; the HFD group was fed a high-fat diet (60% calories from fat, OpenSource Diets™, #D12492, Research Diets Inc; New Brunswick, NJ, USA); and the HFD + Pt group was fed a high-fat diet supplemented with Pt (90 mg/Kg body weight/day). The high-fat diet was smashed, thoroughly mixed with the appropriate amount of Pt (from Waseta Int. Trading Co., Shangai, China), and then compacted again into pellets. Pt amount/g diet was calculated as follows: 90 × mean body weight (Kg)/mean daily diet consumption (g); since body weight changed during the experiment, Pt amount in the diet was increased accordingly during time. To avoid compound degradation, Pt-

supplemented diet was prepared twice a week, stored at 4 °C and changed in animal cages every day. Sample size was determined through power analysis (power = 0.8; effect size = 1.5; α = 0.05). Mice were maintained under the different dietetic regimens for 30 weeks; at the end of this period, they were sacrificed after being fasted for 4 h. Subcutaneous (inguinal) and visceral (epidydimal or periovaric) adipose tissues (sWAT and vWAT, respectively) were collected, immediately frozen in liquid nitrogen and then stored at −80 °C until extraction (see below, Section 2.3).

2.3. RNA and Protein Extraction

RNA and protein extractions were conducted as described in [5]. Briefly, the frozen tissue was grinded in liquid nitrogen with mortar and pestle, and the material was then divided evenly into two test tubes, one for RNA and one for protein extraction.

Total RNA was extracted using the TRIzol reagent (Thermo Fisher Scientific, Waltham, MA, USA) according to the manufacturer's instructions, adding a centrifugation step (5 min at 12,000× *g* at 4 °C) after TRIzol lysis, as recommended by the protocol to remove most of the tissue fat content. RNA content of each sample was quantified with NanoDrop (Thermo Fisher Scientific, Waltham, MA, USA).

Protein extraction was performed by resuspending the frozen tissue powder (about 80 mg) in 0.3 mL RIPA lysis buffer containing protease and phosphatase inhibitors (Merck Life Science S.r.l., Milano, Italy). The samples were incubated for 30 min on ice and then physically disaggregated with an electric pestle (Merck Life Science S.r.l., Milano, Italy). The lysates were then centrifuged at 20,000× *g* for 15 min at 4 °C to remove fat, and finally transferred to a new tube. Quantification of the total protein content in each lysate was performed using the BCA assay (Thermo Fisher Scientific, Waltham, MA, USA).

2.4. Quantitative Real Time PCR (RT-qPCR)

The Superscript VILO reverse transcriptase kit (Thermo Fisher Scientific, Waltham, MA, USA) was used to retro-transcribe 400 ng of total RNA from each sample, following the manufacturer's protocol. Expression levels of target genes were then analyzed by RT-qPCR, using the primers listed in Table 1. All primers were designed with the Primer3 software (version 4.1.0, Whitehead Institute for Biomedical Research, Steve Rozen, Andreas Untergasser, Maido Remm, Triinu Koressaar and Helen Skaletsky, Cambridge, MA, USA). The reactions (8 ng cDNA/reaction) were performed using iQ SYBR Green Supermix (Bio-Rad, Hercules, CA, USA) on a CFX Connect Real-Time System (Bio-Rad, Hercules, CA, USA). All samples were run in triplicate, and *Gapdh* was used as reference gene. Relative gene expression levels were calculated using the $2^{\Delta\Delta Ct}$ method [37].

Table 1. List and sequences of the primers used for RT-qPCR analysis.

Gene	Transcript Accession Number (Ensembl)	Primer
Adiponectin (*Adipoq*)	ENSMUST00000023593.6	F: TGTTCCTCTTAATCCTGCCCA R: CCAACCTGCACAAGTTCCCTT
Cd206 (Mrc1)	ENSMUST00000028045.4	F: TGTGGTGAGCTGAAAGGTGA R: CAGGTGTGGGCTCAGGTAGT
Gapdh	ENSMUST00000073605.15	F: TGTGTCCGTCGTGGATCTGA R: TTGCTGTTGAAGTCGCAGGAG
Il6	ENSMUST00000026845.12	F: CCAGTTGCCTTCTTGGGACT R: GGTCTGTTGGGAGTGGTATCC
Il10	ENSMUST00000016673.6	F: GCTCTTACTGACTGGCATGAG R: CGCAGCTCTAGGAGCATGTG
Tnfα	ENSMUST00000025263.15	F: GTGCCTATGTCTCAGCCTCT R: CTGATGAGAGGGAGGCCATT

2.5. Pt Quantification in the Adipose Tissue

Pterostilbene and metabolites were extracted from sWAT and vWAT as described in [38]. Samples were finally analyzed by high performance liquid chromatography with UV detection (HPLC/UV; 1290 Infinity LC System, Agilent Technologies, Santa Clara, CA, USA) using a reverse phase column (Zorbax Extend-C18, 1.8 μm, 50 × 3.0 mm i.d.; Agilent Technologies) and a UV diode array detector (190–500 nm). Solvents A and B were water containing 0.1% trifluoroacetic acid and acetonitrile, respectively. The gradient for B was as follows: 10% for 0.5 min, then from 10% to 100% in 3.5 min, 100% for 1 min; the flow rate was 0.6 mL/min and the column compartment was maintained at 35 °C. Eluate was preferentially monitored at 286, 300 and 320 nm. Concentration of Pt was determined as described in [38,39].

2.6. Western Blot

Proteins (50 μg for each sample) were separated by SDS-PAGE (Pre-cast NuPAGE 4-12% Bis-Tris Gels, Life Technologies, Carlsbad, CA, USA). After electrophoretic separation, proteins were transferred to PVDF membranes (Immobilion-FL, 0.45 μm, Merk Life Science S.r.l., Milano, Italy). For total protein staining, membranes were incubated for 2–3 min at room temperature with a Pounceau Red 0,5% (*w/v*) solution in 5% (*v/v*) acetic acid (Merck Life Science S.r.l., Milano, Italy), and then rinsed with milliQ water to wash out the background stain. Images of the Pounceau Red staining were acquired in bright field using a UVITEC Eppendorf apparatus. Membranes were then rinsed with milliQ water and destained with Tris-buffered saline buffer supplemented with 0.1% Tween-20 (TBS-T; Merck Life Science S.r.l., Milano, Italy). The membranes were saturated with 5% bovine serum albumin (Merck Life Science S.r.l., Milano, Italy) in TBS-T buffer for 1 h and then incubated overnight at 4 °C with the primary antibody. Primary antibodies used were anti-β-actin (dil. 1:1000; #8457S, Cell Signaling, Danvers, MA, USA), anti-diponectin (dil. 1:1000; #GTX18839, Genetex, Irvine, CA, USA), anti-IL10 (dil. 1:1000; #GTX130512, Genetex, Irvine, CA, USA), anti-phospho-NFkB p65 (Ser 536) (dil. 1:1000; #3033S Cell Signaling, Danvers, MA, USA), anti-NFkB p65 (dil. 1:1000, #8242, Cell Signaling, Danvers, MA, USA), anti-phospho-IkBα (Ser32) (dil. 1:1000, #2859S, Cell Signaling, Danvers, MA, USA), anti-IkBα (dil. 1:1000, #4814S, Cell Signaling, Danvers, MA, USA). The following day, membranes were washed with TBS-T and incubated with horseradish peroxidase-conjugated goat secondary anti-rabbit antibody (#7074, Cell Signaling, Danvers, MA, USA). The chemiluminescence signal was detected using digital imaging by the UVITEC Eppendorf apparatus.

2.7. Statistical Analyses

Statistical analysis was performed using GraphPad Prism Software (version 8, GraphPad Software, San Diego, CA, USA). D'Agostino and Pearson omnibus normality test was performed to assess the normal distribution of the sample population. Comparisons between two groups were performed with Student's *t*-test, when the sample population was normally distributed; otherwise, the non-parametric Mann–Whitney test was performed. Comparisons between three or more groups were performed with Brown–Forsythe and Welch ANOVA tests if data were normally distributed, otherwise with the non-parametric Kruskal–Wallis test. Significance in comparisons was labeled in the figures as follows: * $p \leq 0.05$; ** $p \leq 0.01$; *** $p \leq 0.001$. Spearman's correlation was performed to evaluate the association between gene expression levels.

3. Results

3.1. Effects of Pt on Adiponectin

Since Adiponectin is an adipokine with a crucial role in insulin signalling and browning induction [21,40], we evaluated the alterations in its expression by RT-qPCR in two different WAT depots, namely the sWAT and the vWAT. Compared to the STD group, chronic feeding with high-fat diet (HFD) significantly decreased the expression of *Adiponectin* selectively in the sWAT (Figure 1a). Supplementation with Pt (HFD + Pt group) signif-

icantly increased the *Adiponectin* transcript to levels comparable with those observed in mice fed a standard diet. HFD also decreased the expression of the anti-inflammatory M2-macrophages marker *Cd206*—which was partially reversed by Pt supplementation—and of *Il10*, an anti-inflammatory cytokine produced by M2 macrophages (Figure 1a). In this latter case the Pt-induced "rebound" did not achieve significance, but a trend seemed to be present. Of note, a correlation between the levels of *Adiponectin* and *Il10* transcripts in the sWAT from HFD + Pt mice seems to be present ($p \leq 0.05$, Spearman's correlation coefficient (r) = 0.6; Figure 1d). None of these effects was observed in vWAT (Figure 1b).
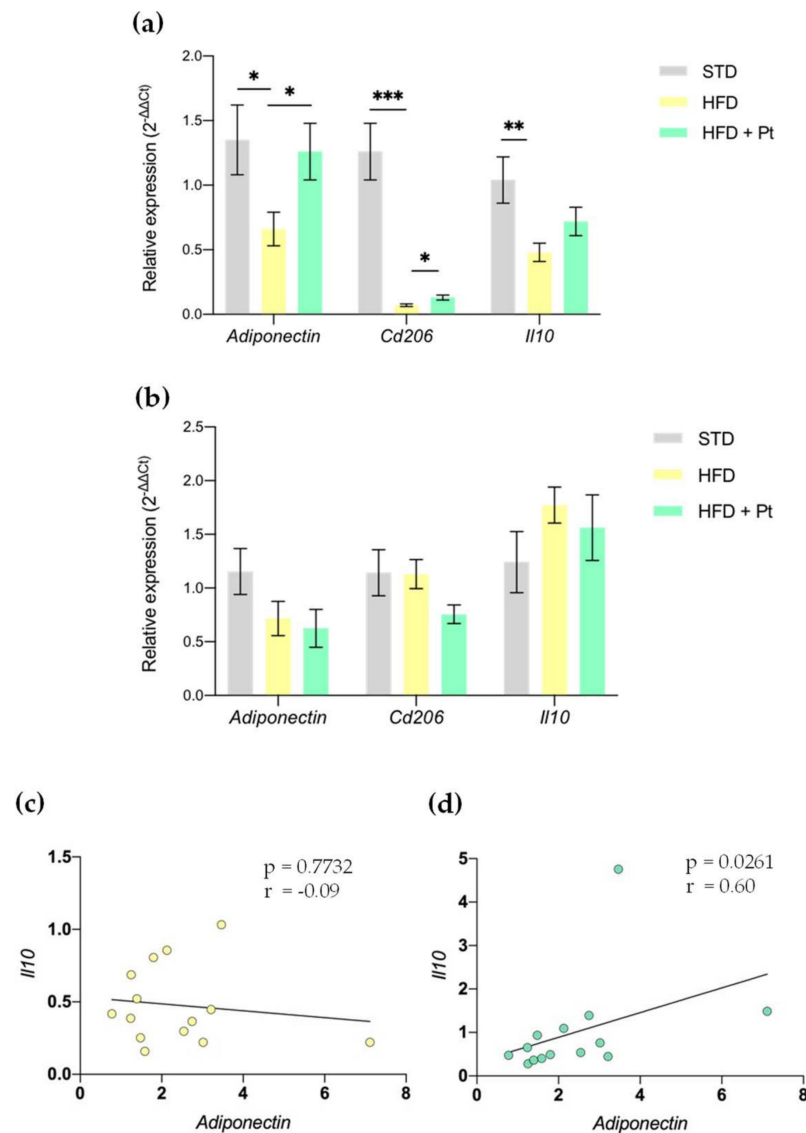
Figure 1. Gene expression analysis of *Adiponectin*, *Cd206*, and *Il10* in sWAT (**a**) and vWAT (**b**) from STD, HFD, and HFD + Pt mice. Mean values ± SEM are shown; data from males and females averaged together. N ≥ 6 for each condition ($n \geq 3$ for males; $n \geq 3$ for females). * $p \leq 0.05$; ** $p \leq 0.01$; *** $p \leq 0.001$. (**c**,**d**): Correlation of *Adiponectin* and *Il10* gene expression in HFD (**c**) and HFD + Pt fed mice (**d**).

Data were also analyzed considering males and females separately (Supplementary Figure S1); since we did not observe sex-dependent differences in the analyzed markers, data from males and females were always averaged and shown together.

To confirm the effect also at the protein level, we performed Western Blot (WB) analysis; since a comparative analysis can be performed only between samples run on the same

blot/gel, and the main focus of the work was to uncover the effects of Pt supplementation, this analysis was performed only on sWAT samples from HFD and HFD + Pt mice. The results confirmed the Pt-driven increase of Adiponectin and IL10 also at the protein level (Figure 2; data considering males and females separately are shown in Supplementary Figure S2).
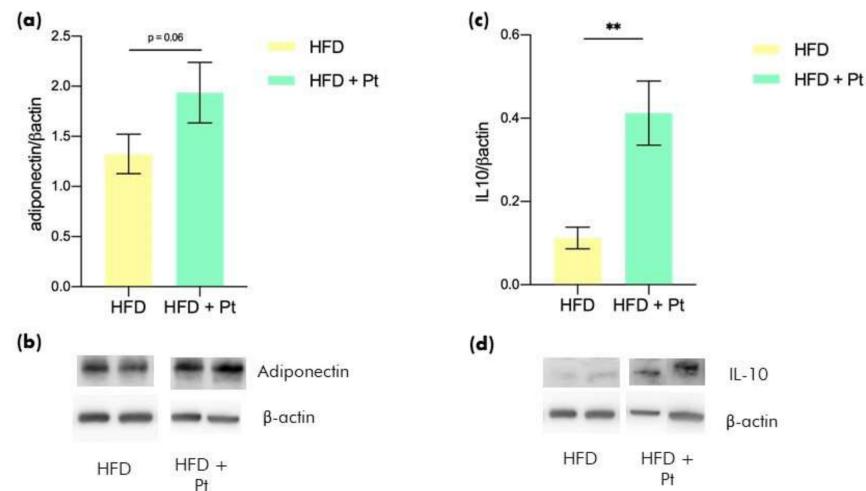

Figure 2. Adiponectin and IL10 protein levels in sWAT from HFD and HFD + Pt mice. (**a,c**): Western Blot quantification; (**b,d**): representative images of WB bands (1 from a male and 1 from a female for each condition). Protein levels were normalized to β-actin. Mean values ± SEM are shown; data from males and females averaged together. $n \geq 8$ for each condition ($n \geq 4$ for males; $n \geq 4$ for females). Statistical analysis was performed using Mann–Whitney test. ** $p \leq 0.01$.

Adiponectin is produced by the adipose tissue and then released in the bloodstream to reach target organs such as liver, muscles, and brain. Thus, we also evaluated by WB analysis the levels of circulating Adiponectin. The results showed no differences between HFD and HFD + Pt mice (Figure 3).
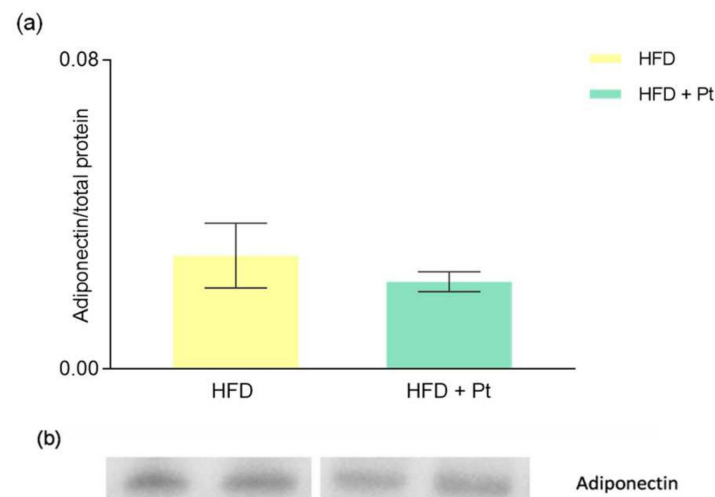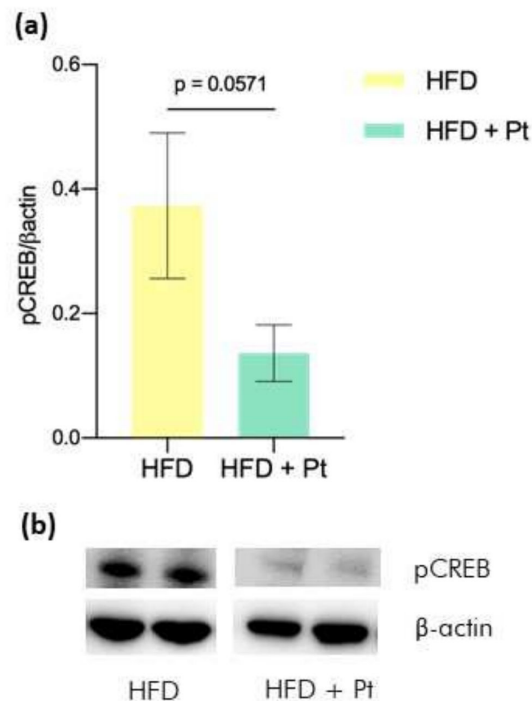

Figure 3. Adiponectin protein levels in serum from HFD and HFD + Pt mice. (**a**) Western Blot quantification. (**b**) representative Western Blot images (1 from a male and 1 from a female for each condition). Adiponectin levels were normalized to the total protein levels of each sample. Mean values ± SEM are shown; data from males and females averaged together. $n \geq 8$ for each condition ($n \geq 4$ for males; $n \geq 4$ for females). Statistical analysis was performed using Mann-Whitney test.

3.2. Effects on CREB

CREB (cAMP response element-binding protein) is a transcription factor that is activated by phosphorylation and promotes the transcription of genes involved in various processes. In the context of obesity, CREB was found to be activated in adipose tissue, where it promotes insulin resistance by triggering expression of the transcriptional repressor ATF3 and thereby downregulating expression of Adiponectin as well as of the insulin-sensitive glucose transporter 4 (GLUT4) [41]. Consistently, we found that Pt supplementation decreased CREB phosphorylation and thus its activation in comparison to the HFD group (Figure 4).

Figure 4. pCREB protein levels in sWAT from HFD and HFD + Pt mice. (**a**) Western Blot quantification; (**b**) representative images of WB bands (1 from a male and 1 from a female for each condition). Protein levels were normalized to β-actin. Mean values ± SEM; data from males and females averaged together. *n* = 4 for each condition (*n* = 2 for males; *n* = 2 for females).

3.3. Pt Quantification in WAT Depots

To exclude a depot-specific effect due to a specific accumulation of Pt, we decided to assess the concentration of Pt and its main Phase II metabolites (i.e., Pt-sulfate and Pt-glucuronide) by HPLC/UV analysis of the vWAT and sWAT from each animal. In most cases, we found negligible levels of Pt metabolites (<0.1 nmoles/g tissue); in only one sample (out of 20 analyzed), Pt-sulfate was detected, at a concentration of 0.5 nmol/g. Non-metabolized/intact Pt was the main specie present in the adipose tissues analyzed. The comparison between sWAT and vWAT did not show any significant difference in Pt accumulation, thus suggesting that the increase observed for *Adiponectin*, *Cd206* and *Il10* in sWAT is not attributable to a higher concentration of the phenol in this depot (Figure 5).
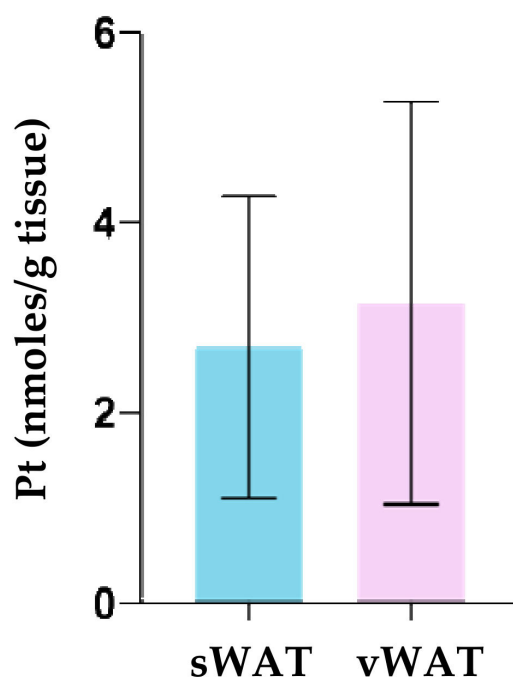
Figure 5. Pterostilbene levels in sWAT and vWAT. Mean values $\pm$ SEM are shown; data from males and females averaged together. $n \geq 6$.

3.4. Effects on Adipose Tissue Inflammation

Since obesity is generally associated with a low-grade chronic inflammation [42], we analyzed the expression of a few pro-inflammatory cytokines (*Tnfα*, *Il6*) and anti-inflammatory *Il10* in the vWAT, which is recognized to be the adipose tissue depot mostly affected by inflammatory processes. However, no significant effects induced by HFD nor by Pt supplementation were observed, aside from a non-significant increase of *Tnfα* gene expression in HFD fed mice compared to the STD group (Figure 6; data considering males and females separately are shown in Supplementary Figure S3). As described in Section 3.1, analysis of the same markers in sWAT revealed that the obesogenic diet caused a reduction of the anti-inflammatory cytokine *Il10* (Figures 1a and 6a), while Pt supplementation increased IL10 levels (Figure 2). Interestingly, we found that Pt paradoxically caused a significant increase of *Tnfα* gene expression. A similar increase has been observed in the serum of mice exposed to cold [29], and thus seems to indicate that the observed increase in *Tnfα* could be part of the browning process induced by Pt. Since pro-inflammatory cytokines are produced as a result of the activation of the NFkB pathway, we also investigated by Western Blot analysis the effects of Pt on the phosphorylation/activation of NFkB and IkBα. Also in this case, as explained in Section 3.1, WB analysis was performed only with WAT samples from HFD and HFD + Pt groups. The results showed that chronic long-term supplementation with Pt did not exert any effect on the NFkB pathway, both in vWAT and sWAT (Figure 7; data considering males and females separately are shown in Supplementary Figures S4 and S5).
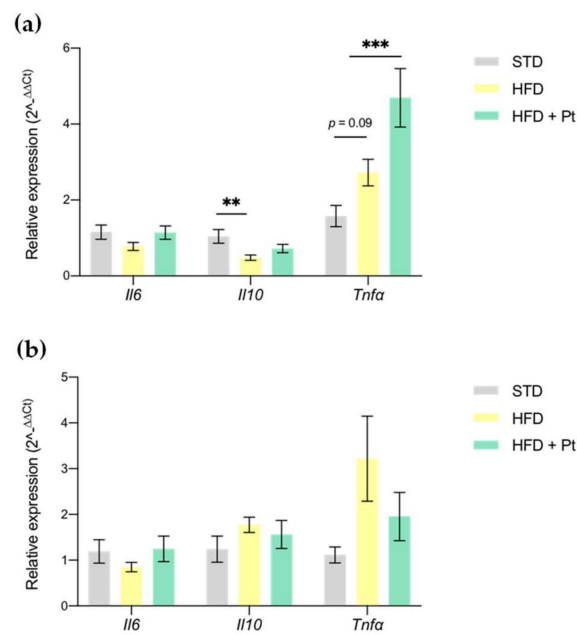
(a)

(b)

Figure 6. Gene expression analysis of *Il6*, *Il10* and *Tnfα* in sWAT (**a**) and vWAT (**b**) from STD, HFD, and HFD + Pt mice. Mean values $\pm$ SEM; data from males and females averaged together. $n \geq 6$ for each condition ($n \geq 3$ for males; $n \geq 3$ for females). ** $p \leq 0.01$; *** $p \leq 0.001$.
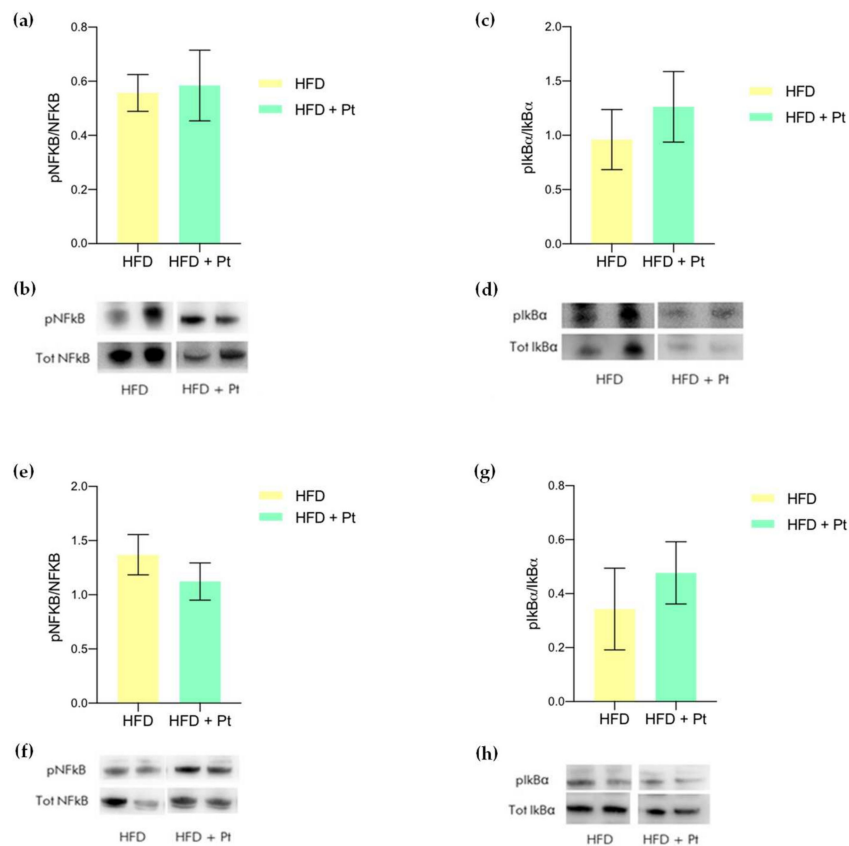
(a) **(c)**

(b) **(d)**

(e) **(g)**

(f) **(h)**

Figure 7. pNFkB and pIKBα protein levels in sWAT (**a–d**) and vWAT (**e–h**) from HFD and HFD + Pt mice. (**a,c,e,g**): Western Blot quantification; (**b,d,f,h**): representative images of WB bands (1 from a male and 1 from a female for each condition). Protein levels were normalized to total NFkB and IKBα. Mean values $\pm$ SEM; data from males and females averaged together. $n \geq 6$ for each condition ($n \geq 3$ for males; $n \geq 3$ for females).

4. Discussion

Although Pt has been already demonstrated to exert multiple beneficial effects on obesity [6–8,43], this study presents some relevant novelties in the field. First, such a long-lasting treatment (30 weeks) had been scarcely investigated so far, with few exceptions concerning for instance effects of the HFD on blood brain barrier function [44], sperm motility [45] and osteogenesis [46]. The long-term supplementation with Pt also supported the lack of toxicity of this natural compound (which was already reported in [47]). Second, males and females were both included in the study: this aspect is particularly important, since females are often underrepresented in the biomedical research with rodents [35,36,48].

The administered dose (90 mg/Kg body weight/day) was selected to ensure Pt levels in the adipose tissue in the 5–10 µM range [5], i.e., in the concentration range at which Pt was demonstrated to exert beneficial effects on adipocytes [49]. This dosage roughly corresponds to a 450 mg daily dose for a 60 Kg person [50]; this is more typical of a dietary supplementation than a dietary intake, since Pt content in blueberries (one of its richest sources) is about 100–520 ng/g [51,52].

We previously published that Pt is able to increase the expression of various genes regulating the browning/beigeing process in the sWAT, such as *Ebf2*, *Sirt1*, *Pgc1α* and *Pparγ* [5]. We demonstrate here that these effects were paralleled by a local increase of Adiponectin and IL10 (both transcript and protein), alongside an increase in the transcription of the marker for M2 anti-inflammatory macrophages *Cd206*. The increase of these markers was selectively observed in the sWAT. The differential effect of Pt on sWAT and vWAT cannot be ascribed to differences in Pt accumulation, since similar Pt levels were detected in sWAT and vWAT (Figure 5). One of the possible causes underlying the observed depot-selective response could be the intrinsic heterogeneity of these white fat depots, each having a specific cellular composition, microenvironment and a unique interaction with stromovascular cells (i.e., macrophages, neutrophils, lymphocytes, fibroblast, and endothelial cells) [53–55].

Our data are consistent with what observed by Hui and co-authors [21]: cold exposure led to a marked increase of Adiponectin both at the transcript and protein levels; also in this case, the accumulation of Adiponectin was selectively observed in sWAT and not in vWAT. The adipokine binds to T-cadherin in M2 macrophages and stimulates their proliferation, skewing the macrophage phenotype distribution towards the anti-inflammatory M2 phenotype. M2 macrophages in turn supply catecholamines for the activation of beige cells [56–58].

Since chronic adipose tissue inflammation is often associated with obesity and is considered to play a major role in the onset of obesity-associated disorders [42], we also analyzed the expression levels of a few pro- and anti-inflammatory markers (*Il6*, *Il10*, and *Tnfα*), both in the vWAT (that is supposed to be the most affected by inflammation), and sWAT. The results obtained from vWAT showed that HFD mice had only a slight increase of *Tnfα* compared to STD mice, and this was partially attenuated by Pt supplementation; none of these variations however reached statistical significance. Evaluation of other markers of inflammation such as *Il6* and *Il10*, as well as the NFkB pathway activation, revealed no effect of the diet or of Pt. Various aspects might contribute to these unexpected results: for example, most of the studies observing an HFD-induced pro-inflammatory effect applied a much shorter feeding protocol than ours. Furthermore, a few reports highlighted that the effects of the diet on low-grade inflammation may be directly correlated to the composition of the diet used [59,60]: feeding mice with very HFD (vHFD) increased weight, fat mass, and plasma and liver triglycerides compared to a low-fat or a moderate-fat diet. However, vHFD-fed mice did not develop metabolic endotoxemia and low-grade inflammation, compared to the other groups. A possible explanation might be found considering intestinal globlet cells and the composition of gut microbiota: the former plays an important role in the modulation of mucus coat composition, while the latter is involved in the frontline host defense against endogenous and exogenous irritants. Indeed, the intestine of vHFD-fed mice was characterized by an increased number of globlet cells, while no changes were observed on gut microbioma composition [59,60]. Finally, the absence of an effect of Pt on

the considered inflammation-related markers might find an explanation in the intervention of adaptive/homeostatic processes, which clearly deserve consideration.

Analysis of the same markers in sWAT, on the other hand, revealed that Pt significantly increased *Tnfα* transcription, when compared to HFD group. Similar results were reported in a few studies studying browning and cold-exposure [29,33]: an increase of several cytokines was reported (*Il6* and *Tnfα* included), and this was hypothesized to play an important role in the cross-talk between WAT and other tissues.

Collectively, our data suggest that Pt could be able to activate sWAT browning through a mechanism likely involving pCREB and Adiponectin. As far as we know, this is the first evidence demonstrating that Pt is able to promote an increase of Adiponectin in vivo.

5. Conclusions

Altogether, the results obtained in this study suggest that Pt might exert a slimming effect through the activation of molecular mechanisms similar to those activated during the physiological response to stimuli such as cold exposure, and culminating in the activation of WAT browning. Indeed, a nutraceutical approach for the prevention of obesity mimicking physiological mechanisms could be advantageous because of the lower risk of side effects, compared to pharmacological agents.

Surprisingly, we did not observe any significant effect of HFD or Pt on vWAT inflammation, suggesting that experimental variables used in preclinical studies, such as diet composition or duration of the treatment, are aspects that deserve attention.

References

1. Koh, Y.C.; Ho, C.T.; Pan, M.H. Recent Advances in Health Benefits of Stilbenoids. *J. Agric. Food Chem.* **2021**, *69*, 10036–10057. [CrossRef] [PubMed]
2. Obrador, E.; Salvador-Palmer, R.; Jihad-Jebbar, A.; López-Blanch, R.; Dellinger, T.H.; Dellinger, R.W.; Estrela, J.M. Pterostilbene in Cancer Therapy. *Antioxidants* **2021**, *10*, 492. [CrossRef] [PubMed]
3. Liu, Y.; You, Y.; Lu, J.; Chen, X.; Yang, Z. Recent Advances in Synthesis, Bioactivity, and Pharmacokinetics of Pterostilbene, an Important Analog of Resveratrol. *Molecules* **2020**, *25*, 5166. [CrossRef] [PubMed]
4. Milton-Laskíbar, I.; Gómez-Zorita, S.; Arias, N.; Romo-Miguel, N.; González, M.; Fernández-Quintela, A.; Portillo, M.P. Effects of resveratrol and its derivative pterostilbene on brown adipose tissue thermogenic activation and on white adipose tissue browning process. *J. Physiol. Biochem.* **2020**, *76*, 269–278. [CrossRef]
5. La Spina, M.; Galletta, E.; Azzolini, M.; Gomez Zorita, S.; Parrasia, S.; Salvalaio, M.; Salmaso, A.; Biasutto, L. Browning Effects of a Chronic Pterostilbene Supplementation in Mice Fed a High-Fat Diet. *Int. J. Mol. Sci.* **2019**, *20*, 5377. [CrossRef] [PubMed]
6. Gómez-Zorita, S.; González-Arceo, M.; Trepiana, J.; Aguirre, L.; Crujeiras, A.B.; Irles, E.; Segues, N.; Bujanda, L.; Portillo, M.P. Comparative Effects of Pterostilbene and Its Parent Compound Resveratrol on Oxidative Stress and Inflammation in Steatohepatitis Induced by High-Fat High-Fructose Feeding. *Antioxidants* **2020**, *9*, 1042. [CrossRef]
7. Gómez-Zorita, S.; Milton-Laskibar, I.; Macarulla, M.T.; Biasutto, L.; Fernández-Quintela, A.; Miranda, J.; Lasa, A.; Segues, N.; Bujanda, L.; Portillo, M.P. Pterostilbene modifies triglyceride metabolism in hepatic steatosis induced by high-fat high-fructose feeding: A comparison with its analog resveratrol. *Food Funct.* **2021**, *12*, 3266–3279. [CrossRef]
8. Gómez-Zorita, S.; Milton-Laskíbar, I.; Aguirre, L.; Fernández-Quintela, A.; Xiao, J.; Portillo, M.P. Effects of Pterostilbene on Diabetes, Liver Steatosis and Serum Lipids. *Curr. Med. Chem.* **2021**, *28*, 238–252. [CrossRef]
9. Shinde, A.B.; Song, A.; Wang, Q.A. Brown Adipose Tissue Heterogeneity, Energy Metabolism, and Beyond. *Front. Endocrinol.* **2021**, *12*, 651763. [CrossRef]
10. Maliszewska, K.; Kretowski, A. Brown Adipose Tissue and Its Role in Insulin and Glucose Homeostasis. *Int. J. Mol. Sci.* **2021**, *22*, 1530. [CrossRef]
11. Wang, C.H.; Wei, Y.H. Therapeutic Perspectives of Thermogenic Adipocytes in Obesity and Related Complications. *Int. J. Mol. Sci.* **2021**, *22*, 7177. [CrossRef] [PubMed]
12. Verduci, E.; Calcaterra, V.; Di Profio, E.; Fiore, G.; Rey, F.; Magenes, V.C.; Todisco, C.F.; Carelli, S.; Zuccotti, G.V. Brown Adipose Tissue: New Challenges for Prevention of Childhood Obesity. A Narrative Review. *Nutrients* **2021**, *13*, 1450. [CrossRef] [PubMed]
13. Symonds, M.E.; Pope, M.; Bloor, I.; Law, J.; Alagal, R.; Budge, H. Adipose tissue growth and development: The modulating role of ambient temperature. *J. Endocrinol.* **2021**, *248*, R19–R28. [CrossRef] [PubMed]
14. Motta, V.F.; Bargut, T.L.; Souza-Mello, V.; Aguila, M.B.; Mandarim-de-Lacerda, C.A. Browning is activated in the subcutaneous white adipose tissue of mice metabolically challenged with a high-fructose diet submitted to high-intensity interval training. *J. Nutr. Biochem.* **2019**, *70*, 164–173. [CrossRef] [PubMed]
15. Atakan, M.M.; Koşar, Ş.N.; Güzel, Y.; Tin, H.T.; Yan, X. The Role of Exercise, Diet, and Cytokines in Preventing Obesity and Improving Adipose Tissue. *Nutrients* **2021**, *13*, 1459. [CrossRef] [PubMed]
16. Volke, L.; Krause, K. Effect of Thyroid Hormones on Adipose Tissue Flexibility. *Eur. Thyroid J.* **2021**, *10*, 1–9. [CrossRef]
17. Sentis, S.C.; Oelkrug, R.; Mittag, J. Thyroid hormones in the regulation of brown adipose tissue thermogenesis. *Endocr. Connect.* **2021**, *10*, R106–R115. [CrossRef]
18. Tabuchi, C.; Sul, H.S. Signaling Pathways Regulating Thermogenesis. *Front. Endocrinol.* **2021**, *12*, 595020. [CrossRef]
19. Zhang, Z.; Yang, D.; Xiang, J.; Zhou, J.; Cao, H.; Che, Q.; Bai, Y.; Guo, J.; Su, Z. Non-shivering Thermogenesis Signalling Regulation and Potential Therapeutic Applications of Brown Adipose Tissue. *Int. J. Biol. Sci.* **2021**, *17*, 2853–2870. [CrossRef]
20. Lu, K.Y.; Primus Dass, K.T.; Tsai, S.F.; Chuang, H.M.; Lin, S.Z.; Liu, S.P.; Harn, H.J. Clinical Application Potential of Small Molecules that Induce Brown Adipose Tissue Thermogenesis by Improving Fat Metabolism. *Cell Transplant.* **2020**, *29*, 1–13. [CrossRef]
21. Hui, X.; Gu, P.; Zhang, J.; Nie, T.; Pan, Y.; Wu, D.; Feng, T.; Zhong, C.; Wang, Y.; Lam, K.S.; et al. Adiponectin Enhances Cold-Induced Browning of Subcutaneous Adipose Tissue via Promoting M2 Macrophage Proliferation. *Cell Metab.* **2015**, *22*, 279–290. [CrossRef] [PubMed]
22. Wei, Q.; Lee, J.H.; Wang, H.; Bongmba, O.Y.N.; Wu, C.S.; Pradhan, G.; Sun, Z.; Chew, L.; Bajaj, M.; Chan, L.; et al. Adiponectin is required for maintaining normal body temperature in a cold environment. *BMC Physiol.* **2017**, *17*, 8. [CrossRef] [PubMed]
23. Lee, M.J.; Wu, Y.; Fried, S.K. Adipose tissue heterogeneity: Implication of depot differences in adipose tissue for obesity complications. *Mol. Asp. Med.* **2013**, *34*, 1–11. [CrossRef] [PubMed]
24. García, M.D.C.; Pazos, P.; Lima, L.; Diéguez, C. Regulation of Energy Expenditure and Brown/Beige Thermogenic Activity by Interleukins: New Roles for Old Actors. *Int. J. Mol. Sci.* **2018**, *19*, 2569. [CrossRef]
25. Qiu, Y.; Nguyen, K.D.; Odegaard, J.I.; Cui, X.; Tian, X.; Locksley, R.M.; Palmiter, R.D.; Chawla, A. Eosinophils and type 2 cytokine signaling in macrophages orchestrate development of functional beige fat. *Cell* **2014**, *157*, 1292–1308. [CrossRef]
26. Lee, M.W.; Odegaard, J.I.; Mukundan, L.; Qiu, Y.; Molofsky, A.B.; Nussbaum, J.C.; Yun, K.; Locksley, R.M.; Chawla, A. Activated type 2 innate lymphoid cells regulate beige fat biogenesis. *Cell* **2015**, *160*, 74–87. [CrossRef]
27. Catrysse, L.; van Loo, G. Inflammation and the Metabolic Syndrome: The Tissue-Specific Functions of NF-kappaB. *Trends Cell Biol.* **2017**, *27*, 417–429. [CrossRef]

28. Saltiel, A.R.; Olefsky, J.M. Inflammatory mechanisms linking obesity and metabolic disease. *J. Clin. Investig.* **2017**, *127*, 1–4. [CrossRef]

29. Bal, N.C.; Maurya, S.K.; Pani, S.; Sethy, C.; Banerjee, A.; Das, S.; Patnaik, S.; Kundu, C.N. Mild cold induced thermogenesis: Are BAT and skeletal muscle synergistic partners? *Biosci. Rep.* **2017**, *37*, BSR20171087. [CrossRef]

30. Xu, B.; Lian, S.; Li, S.Z.; Guo, J.R.; Wang, J.F.; Wang, D.; Zhang, L.P.; Yang, H.M. GABAB receptor mediate hippocampal neuroinflammation in adolescent male and female mice after cold expose. *Brain Res. Bull.* **2018**, *142*, 163–175. [CrossRef]

31. Wernstedt, I.; Edgley, A.; Berndtsson, A.; Fäldt, J.; Bergström, G.; Wallenius, V.; Jansson, J.O. Reduced stress- and cold-induced increase in energy expenditure in interleukin-6-deficient mice. *Am. J. Physiol. Regul. Integr. Comp. Physiol.* **2006**, *291*, R551–R557. [CrossRef] [PubMed]

32. Knudsen, J.G.; Murholm, M.; Carey, A.L.; Biensø, R.S.; Basse, A.L.; Allen, T.L.; Hidalgo, J.; Kingwell, B.A.; Febbraio, M.A.; Hansen, J.B.; et al. Role of IL-6 in exercise training- and cold-induced UCP1 expression in subcutaneous white adipose tissue. *PLoS ONE* **2014**, *9*, e84910. [CrossRef] [PubMed]

33. Egecioglu, E.; Anesten, F.; Schéle, E.; Palsdottir, V. Interleukin-6 is important for regulation of core body temperature during long-term cold exposure in mice. *Biomed. Rep.* **2018**, *9*, 206–212. [CrossRef] [PubMed]

34. Vasconcelos, R.P.; Peixoto, M.S.; de Oliveira, K.A.; Ferreira, A.C.F.; Coelho-de-Souza, A.N.; Carvalho, D.P.; de Oliveira, A.C.; Fortunato, R.S. Sex differences in subcutaneous adipose tissue redox homeostasis and inflammation markers in control and high-fat diet fed rats. *Appl. Physiol. Nutr. Metab.* **2019**, *44*, 720–726. [CrossRef]

35. Prendergast, B.J.; Onishi, K.G.; Zucker, I. Female mice liberated for inclusion in neuroscience and biomedical research. *Neurosci. Biobehav. Rev.* **2014**, *40*, 1–5. [CrossRef]

36. Clayton, J.A.; Collins, F.S. Policy: NIH to balance sex in cell and animal studies. *Nature* **2014**, *509*, 282–283. [CrossRef]

37. Livak, K.J.; Schmittgen, T.D. Analysis of relative gene expression data using real-time quantitative PCR and the 2(-Delta Delta C(T)) Method. *Methods* **2001**, *25*, 402–408. [CrossRef]

38. Mattarei, A.; Rossa, A.; Bombardelli, V.; Azzolini, M.; La Spina, M.; Paradisi, C.; Zoratti, M.; Biasutto, L. Novel lipid-mimetic prodrugs delivering active compounds to adipose tissue. *Eur. J. Med. Chem.* **2017**, *135*, 77–88. [CrossRef]

39. Azzolini, M.; La Spina, M.; Mattarei, A.; Paradisi, C.; Zoratti, M.; Biasutto, L. Pharmacokinetics and tissue distribution of pterostilbene in the rat. *Mol. Nutr. Food Res.* **2014**, *58*, 2122–2132. [CrossRef]

40. Iwabu, M.; Okada-Iwabu, M.; Yamauchi, T.; Kadowaki, T. Adiponectin/AdipoR Research and Its Implications for Lifestyle-Related Diseases. *Front. Cardiovasc. Med.* **2019**, *6*, 116. [CrossRef]

41. Qi, L.; Saberi, M.; Zmuda, E.; Wang, Y.; Altarejos, J.; Zhang, X.; Dentin, R.; Hedrick, S.; Bandyopadhyay, G.; Hai, T.; et al. Adipocyte CREB promotes insulin resistance in obesity. *Cell Metab.* **2009**, *9*, 277–286. [CrossRef] [PubMed]

42. Kawai, T.; Autieri, M.V.; Scalia, R. Adipose tissue inflammation and metabolic dysfunction in obesity. *Am. J. Physiol. Cell Physiol.* **2021**, *320*, C375–C391. [CrossRef] [PubMed]

43. Gomez-Zorita, S.; Fernandez-Quintela, A.; Lasa, A.; Aguirre, L.; Rimando, A.M.; Portillo, M.P. Pterostilbene, a dimethyl ether derivative of resveratrol, reduces fat accumulation in rats fed an obesogenic diet. *J. Agric. Food Chem.* **2014**, *62*, 8371–8378. [CrossRef] [PubMed]

44. Takechi, R.; Pallebage-Gamarallage, M.M.; Lam, V.; Giles, C.; Mamo, J.C. Nutraceutical agents with anti-inflammatory properties prevent dietary saturated-fat induced disturbances in blood-brain barrier function in wild-type mice. *J. Neuroinflamm.* **2013**, *10*, 73. [CrossRef]

45. Fernandez, C.D.; Bellentani, F.F.; Fernandes, G.S.; Perobelli, J.E.; Favareto, A.P.; Nascimento, A.F.; Cicogna, A.C.; Kempinas, W.D. Diet-induced obesity in rats leads to a decrease in sperm motility. *Reprod. Biol. Endocrinol.* **2011**, *9*, 32. [CrossRef]

46. Tauer, J.T.; Boraschi-Diaz, I.; Al Rifai, O.; Rauch, F.; Ferron, M.; Komarova, S.V. Male but not female mice with severe osteogenesis imperfecta are partially protected from high-fat diet-induced obesity. *Mol. Genet. Metab.* **2021**, *133*, 211–221. [CrossRef]

47. Ruiz, M.J.; Fernandez, M.; Pico, Y.; Manes, J.; Asensi, M.; Carda, C.; Asensio, G.; Estrela, J.M. Dietary administration of high doses of pterostilbene and quercetin to mice is not toxic. *J. Agric. Food Chem.* **2009**, *57*, 3180–3186. [CrossRef]

48. Clayton, J.A. Studying both sexes: A guiding principle for biomedicine. *FASEB J. Off. Publ. Fed. Am. Soc. Exp. Biol.* **2016**, *30*, 519–524. [CrossRef]

49. Hsu, C.L.; Lin, Y.J.; Ho, C.T.; Yen, G.C. Inhibitory effects of garcinol and pterostilbene on cell proliferation and adipogenesis in 3T3-L1 cells. *Food Funct.* **2012**, *3*, 49–57. [CrossRef]

50. Nair, A.B.; Jacob, S. A simple practice guide for dose conversion between animals and human. *J. Basic Clin. Pharm.* **2016**, *7*, 27–31. [CrossRef]

51. Rimando, A.M.; Kalt, W.; Magee, J.B.; Dewey, J.; Ballington, J.R. Resveratrol, pterostilbene, and piceatannol in vaccinium berries. *J. Agric. Food Chem.* **2004**, *52*, 4713–4719. [CrossRef] [PubMed]

52. Neto, C.C. Cranberry and blueberry: Evidence for protective effects against cancer and vascular diseases. *Mol. Nutr. Food Res.* **2007**, *51*, 652–664. [CrossRef] [PubMed]

53. Luong, Q.; Huang, J.; Lee, K.Y. Deciphering White Adipose Tissue Heterogeneity. *Biology* **2019**, *8*, 23. [CrossRef] [PubMed]

54. Sackmann-Sala, L.; Berryman, D.E.; Munn, R.D.; Lubbers, E.R.; Kopchick, J.J. Heterogeneity among white adipose tissue depots in male C57BL/6J mice. *Obesity* **2012**, *20*, 101–111. [CrossRef] [PubMed]

55. Caesar, R.; Manieri, M.; Kelder, T.; Boekschoten, M.; Evelo, C.; Muller, M.; Kooistra, T.; Cinti, S.; Kleemann, R.; Drevon, C.A. A combined transcriptomics and lipidomics analysis of subcutaneous, epididymal and mesenteric adipose tissue reveals marked functional differences. *PloS ONE* **2010**, *5*, e11525. [CrossRef] [PubMed]

56. Parker-Duffen, J.L.; Nakamura, K.; Silver, M.; Kikuchi, R.; Tigges, U.; Yoshida, S.; Denzel, M.S.; Ranscht, B.; Walsh, K. T-cadherin is essential for adiponectin-mediated revascularization. *J. Biol. Chem.* **2013**, *288*, 24886–24897. [CrossRef]

57. Nakatsuji, H.; Kishida, K.; Sekimoto, R.; Komura, N.; Kihara, S.; Funahashi, T.; Shimomura, I. Accumulation of adiponectin in inflamed adipose tissues of obese mice. *Metab. Clin. Exp.* **2014**, *63*, 542–553. [CrossRef]

58. Denzel, M.S.; Scimia, M.C.; Zumstein, P.M.; Walsh, K.; Ruiz-Lozano, P.; Ranscht, B. T-cadherin is critical for adiponectin-mediated cardioprotection in mice. *J. Clin. Investig.* **2010**, *120*, 4342–4352. [CrossRef]

59. Benoit, B.; Laugerette, F.; Plaisancié, P.; Géloën, A.; Bodennec, J.; Estienne, M.; Pineau, G.; Bernalier-Donadille, A.; Vidal, H.; Michalski, M.C. Increasing fat content from 20 to 45 wt% in a complex diet induces lower endotoxemia in parallel with an increased number of intestinal goblet cells in mice. *Nutr. Res.* **2015**, *35*, 346–356. [CrossRef]

60. Benoit, B.; Plaisancié, P.; Awada, M.; Géloën, A.; Estienne, M.; Capel, F.; Malpuech-Brugère, C.; Debard, C.; Pesenti, S.; Morio, B.; et al. High-fat diet action on adiposity, inflammation, and insulin sensitivity depends on the control low-fat diet. *Nutr. Res.* **2013**, *33*, 952–960. [CrossRef]